



DECEMBER 2004
VOL. 15, NO. 1

Newsletter of the SPIE Electronic Imaging Technical Group

Gabriel Marcu, Apple Computer, Inc.
Editor/Technical Group Chair

Special Issue on:
Multi-Spectral Imaging

ELECTRONIC IMAGING

Spectral sensitivity functions for humans and imagers: 1861 to 2004

John J. McCann, McCann Imaging

Contents

Do we really need spectral imaging?, Jussi Parkkinen and Timo Jaaskelainen, University of Joensuu; Esa Torniainen, M-real Corporation 2

Spectral imaging at Chiba University: past, present and future, Prof. Yoichi Miyake, Director of Research Center for Frontier Medical Engineering, Chiba University 3

Estimation of fluorescent scene illuminant using spectral imaging, Shoji Tominaga, Department of Engineering Informatics, Osaka Electro-Communication University 4

Challenges in color reproduction: towards higher dimensions, Raja Bala, Principal Scientist, Xerox Imaging and Services Technology Center 5

Effects of spectral information changes on spatial color computation, Alessandro Rizzi, Dipartimento di Tecnologie dell'Informazione Università degli Studi di Milano; Davide Gadia and Daniele Marini, Dipartimento di Informatica e Comunicazione Università degli Studi di Milano 6

Acquiring and calibrating a large-dynamic-range image database of natural scenes, Fuhui Long, Center for Cognitive Neuroscience, Duke University; Hanchuan Peng, Life Sciences Division, Lawrence Berkeley National Laboratory 7

Segmentation for mixed raster contents with multiple extracted constant-color areas, Zhigang Fan and Timothy Jacobs, Xerox Corporation 12

Four distinct scientific disciplines have contributed to our understanding of sensitivity to wavelengths between 400 and 700nm, both for human vision and color imagers. These are physics, physiology, psychophysics, and the practical engineering of image making.

History of color sensitivity functions

There are many different three-channel color sensitivity functions. They fall into two distinct groups: narrow, non-overlapping curves used by image makers; and broad, overlapping curves derived from characterizing human vision. J. C. Maxwell described both in the 1860s. He was the first photographic color image maker. His color-matching equations from spinning disc measurements and his sensitivity functions from monochromator data are the predecessors of all CIE colorimetric standards.

In 1889 Frederick Ives tried to combine Maxwell's two ideas. He proposed that the color separations used to make reproductions would have the most 'natural' color if the separations had the same spectral sensitivities as humans. He published a book and filed a US patent.¹ Despite a significant investment in the idea of using broad sensitivity functions, Ives abandoned the idea and used narrow-band filters in his 1895 Kromstop color cameras.

Crosstalk

Color-channel crosstalk² is the biggest difference between the narrow, non-overlapping sensitivity functions of practical imaging and the broad, overlapping sensitivities of human vision. Let us consider three colors of paper—white, gray, and red—illuminated by three narrow-band LEDs at 625nm, 530nm and 455nm. The total long-wave response

(TLR) is:

$$TLR = [(I_{625} \times R_{625} \times LS_{625}) + (I_{530} \times R_{530} \times LS_{530}) + (I_{455} \times R_{455} \times LS_{455})]$$

where I is the incident illumination, R is the % reflectance and LS is the long-wave channel's sensitivity for each wavelength used. The long-wave sensors' primary response is to 625nm: at 530nm and 455nm the response is crosstalk.

Imaging systems minimize crosstalk as much as possible. With no crosstalk $LS_{530} = 0$ and $LS_{455} = 0$, then the $TLR = (I_{625} \times R_{625} \times LS_{625})$, limited to the primary response. The white paper has $R_{625} = 90\%$, $R_{530} = 90\%$, $R_{455} = 90\%$; the red paper has $R_{625} = 90\%$, $R_{530} = 12\%$, $R_{455} = 8\%$. The TLR of both white and red papers is $(0.9 \times I_{625} \times LS_{625})$.

The broad human sensitivities generate substantial crosstalk; the red paper shows a significant change in responses with illumination. With crosstalk, the TLR is the combination of 90%, 12% and 8% reflectances in the proportions determined by the values of I and LS. Substantial increases in 530nm and 455nm illuminants relative to 625nm reduce the fraction of primary response in the TLR. The effect of crosstalk is to reduce the chroma of the red paper. The amount of reduction depends on the proportions of the illuminants. Parallel analyses hold for all color channels.

Despite the seductiveness of Ives's 'natural color' idea, all reproduction processes avoid crosstalk because it severely limits color gamut. As shown above, spectral crosstalk compresses the range of chromatic colors. At the receptor stage, the achromatic scale from white to black has a greater range

Continues on page 8.

Do we really need spectral imaging?

Jussi Parkkinen and Timo Jaaskelainen, University of Joensuu; Esa Tornainen, M-real Corporation

Color science is one of a number that has been around since the ancient Greeks. The earliest theories about color naturally related to the prevalent view of nature at the time: color was understood as a substance coming from an object to the eye. Newton was the first who showed and understood the spectral theory of color. He discovered that, for instance, white is not one of the primary colors, but a combination of separate hues. These hues correspond to different wavelengths of electromagnetic radiation, including light, and the wavelength distribution can be expressed as a color spectrum.

In practice, light from all natural objects has some intensity of all wavelengths, so the observed color is dependent on the relative distribution of wavelengths in the spectrum.

This understanding of the real physical nature of color lead to developments in the understanding of human color vision in late-19th early-20th centuries. The human vision model is based on the fact that there are three types of color-sensitive cells, cones, in the human retina. Each of these has a slightly different light-sensitivity function than the others. For this reason, the color signal—i.e. the spectrum—is represented as three values in the human visual system. This is the basis for all standard three-dimensional color-coordinate systems, which can be derived from the theoretically-defined human tristimulus values. These standard color representations are widely used in industry as references in quality control: for producing colors either on digital or printed media, or in color measurement systems etc.

So, when do we need spectral color?

Spectral color, also referred as multispectral color, means the representation of color in the form of a spectrum rather than three values. The idea is to preserve in the color measurement and process as much information as possible. The spectrum carries all the information that produces the human color sensation when the light reaches the eye, and is therefore the most basic way to represent color. All the standard three-dimensional representations can be computed from the spectrum.

Figure 1 shows an example where a spec-

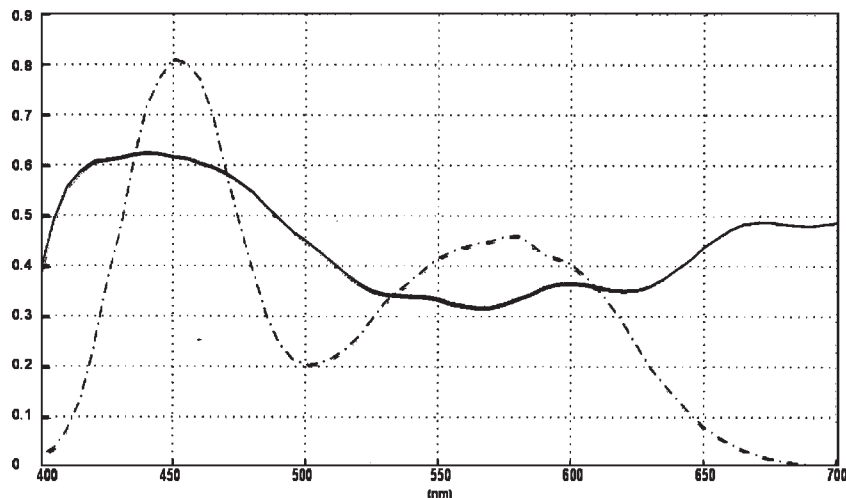


Figure 1. Two metamer spectra that look the same in daylight, but different under tungsten bulb illumination.

trum is needed. There are two color spectra from two different objects. The standard CIELAB values under daylight illumination are the same for both of the spectra: $L^* = 66.90$, $a^* = 11.94$, and $b^* = -24.60$. Under tungsten bulb illumination, the standard CIELAB-values are: $L^* = 66.37$, $a^* = 5.27$, and $b^* = -24.16$ for one spectrum and $L^* = 66.51$, $a^* = -5.80$, and $b^* = -22.84$ for the other. For example, here we need spectral color representation in order to get better quality control in production. When the color quality is defined by standard CIELAB coordinate system, even high-quality requirements can be reached in principle, but not in practice, due to this possibility of difference in the spectrum. The example above could have a practical use in the paper or textile industry, where customers set color-quality requirements in CIELAB values under daylight illumination, but the actual products are viewed in a room with tungsten bulb illumination. This can be the case in the paper industry for different production sets, and in the textile industry for separate garments produced in different factories.

In the printing industry, the need for spectral color is also clear. Color printing can be tuned better using spectral approach and the new generation of printers will use more colors. Such printer will also need the spectral approach for reasonable color management. Finally, in the digital world, the spectral approach allows us to manage and show colors as accurately as possible, so that the ambient illumination can be taken into account. This provides

opportunities for digital proofing in printing industry and high-quality color reproduction in e-Commerce and in telemedicine.

In general one can say that, in three-dimensional coordinate systems such as RGB, one can produce nice-looking and beautiful colors and color images. However, only by using the spectral approach can one produce the *correct* colors and color images. As one of our industrial partners said, "Using only standard three-dimensional color-coordinate systems and no color spectra is like developing Formula 1 racing cars based on noise and exhaust."

So, perhaps the real question is, "Do we really need three-dimensional color coordinate systems?"

Jussi Parkkinen, Timo Jaaskelainen, and Esa Tornainen*

University of Joensuu, Joensuu, Finland

E-mail: Jussi.Parkkinen@cs.joensuu.fi

*M-real Corporation

Virkkala, Finland

Tell us about your news, ideas, and events!

If there are things you'd like to see us cover in the newsletter, please let our Technical Editor, Sunny Bains (sunny@spie.org) know by the deadline date indicated below. Before submitting an article, please check out our full submission guidelines at:

<http://www.sunnybains.com/newslet.html>

Special issues

Proposals for topical issues are welcomed and should include:

- A brief summary of the proposed topic;
- The reason why it is of current interest;
- A brief resumé of the proposed guest editor.

Special issue proposals should be submitted, by the deadline, to Sunny Bains and will be reviewed by the Technical group Chair.

Upcoming deadlines

21 January 2005: Special issue proposals.

4 February 2005: Ideas for articles you'd like to write (or read).

25 March 2005: Calendar items for the 12 months starting **June 2005**.

Spectral imaging at Chiba University: past, present and future

Prof. Yoichi Miyake, Director of Research Center for Frontier Medical Engineering, Chiba University

In general, the quality of an image is determined by sharpness, tone-reproduction characteristics, color reproduction, graininess, texture, gross distortion, and so on. We consider here the color reproduction characteristics of an object, which is dependent on many factors. These include the spectral characteristics of the illumination during both image acquisition and viewing, and those of imaging system. Recording the spectral reflectance of the object will ensure that the color reproduction of the object is independent of illumination. However, this places special demands on both imaging acquisition and color reproduction systems.

For a decade, such color management has been required for device-independent color reproduction and color transformation between different imaging systems. As a result, spectral recording and reproduction methods based on object reflectance spectra have been taken up by many scientists in preference to the conventional colorimetric method based on tri-stimulus values.

In 1988, we developed a new endoscopic spectrophotometer for measuring the spectral reflectance of the gastric mucous membrane in cooperation with Olympus Optical Co. Ltd.. Figure 1 shows the block diagram of this device. We used this to acquire spectra from many different subjects, and the spectral reflectance of the membranes tested were analyzed using principal component analysis. The results indicated that the reflectance spectra of many of these could be adequately described using just three principal components: including human skin.

Based on these experimental results, we showed that the reflectance spectra of all pixels representing the gastric mucous membrane or human skin could be calculated from the RGB signals taken using our electronic endoscope and CCD camera. It thus became possible to improve the color reproduction of

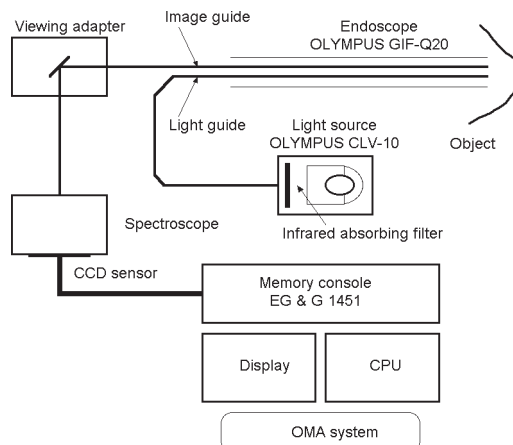


Figure 1. Block diagram of the endoscopic spectrophotometer.

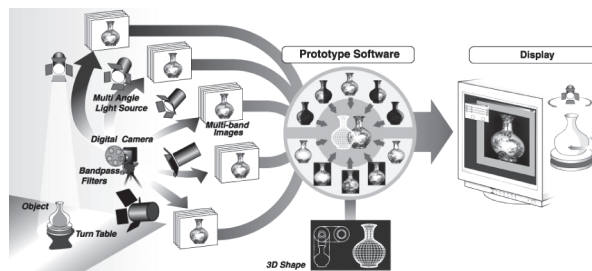


Figure 2. Schematic diagram of the gonio-spectral imaging system.

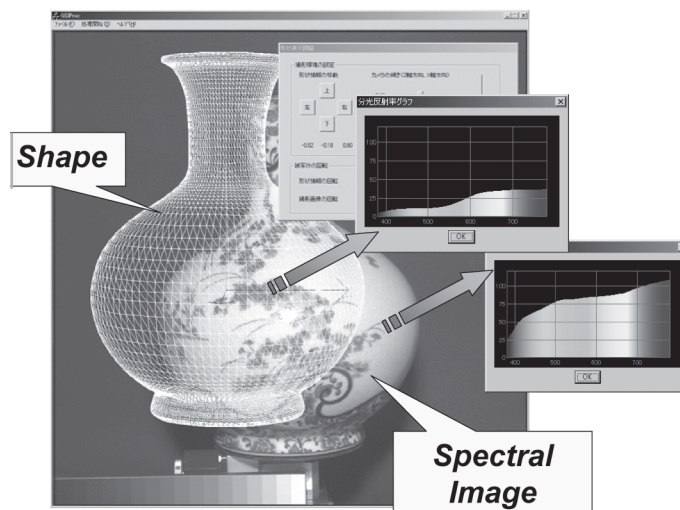


Figure 3. Three-dimensional representation of the object with information about both shape and spectral reflectance.

these objects in various kinds of imaging systems using computer simulation techniques. For example, we were able to optimize the spectral transmittance of separation filters for improving the image capture of the gastric mucous membrane. Using spectral printing, it was also possible to do spectral color reproduction of the acquired images to improve color rendition in different illumination and viewing conditions.

For applications in the arts, in 1997 we developed a multi-band camera to record the reflectance spectra of paintings based on principal-component analysis and Wiener estimation method. The camera consists of a single chip CCD with a rotating color wheel comprising five filters. This camera was effectively used to acquire digital archives, as well as for fundamental research on spectral imaging. We also developed gonio-spectral imaging systems (see Figure 2) that allow us to simultaneously record the spectral and shape information of three-dimensional objects (see Figure 3).

In addition to developing systems, in 1999 we organized the first international conference on multispectral imaging. Since then, the International Conference on Multispectral Imaging (MSI) has become an annual event. It was held at Chiba University again in 2000, then at the University of Joensuu, in Tokyo, in Rochester, and in Aachen. Future events are planned for Granada in 2005 and San Jose in 2006.

We believe that the spectral imaging has many applications in science, technology, and industry and our results show only the beginning of these possibilities. We look forward to extending our cooperation to many international organizations and companies, and hope that many more fields of ap-

Continues on page 8.

Estimation of fluorescent scene illuminant using spectral imaging

Shoji Tominaga, Department of Engineering Informatics, Osaka Electro-Communication University

Most studies on the problem of estimating scene illumination assume a continuous spectral-power distribution like that of an incandescent lamp light or natural daylight.¹ Illuminants with spectral-power distributions that include spikes, such as fluorescent lighting, have thus been neglected. The spectral distribution of a such a lamp shows strong spectral lines together with a weaker, continuous portion of the spectrum. Illuminant spectra with spikes cannot be represented at all when using linear models with smooth basis functions.

The illuminant classification approach is useful for inferring scene illumination with a spiky spectrum.² We have proposed a method of classifying fluorescent scene illumination using a spectral-camera system with narrow-band filtration. The spectral shape is decomposed into two parts—spikes and continuum—that correspond, respectively, to the bright-line and background-continuous spectra. We note that wavelengths of the line spectrum are inherent to the fluorescent material used in the lamp, so it is possible to infer the material class of fluorescent light source by knowing the wavelength positions of spikes on the observed illuminant spectrum.

Spectral camera

The system is composed of a liquid-crystal tunable (LCT) filter, a monochrome CCD camera, and a personal computer. We sample the visible wavelength range (400-700nm) at intervals of 5nm, acquiring monochromatic images at 61 wavelengths. Moreover, we capture additional images at eight wavelengths that correspond to the bright lines of the most common fluorescent lamps. Figure 1 shows the spectral-sensitivity functions of the camera system. The bold curves in Figure 1 represent the additional sensor responses. The resulting spectral image therefore consists of a set of 69 monochrome images.

Basic algorithm

The spectral curve of the fluorescent light is divided into several peak areas and a background continuum. The set of the peak wavelengths found provides the key to identifying the unknown fluorescent light source when we

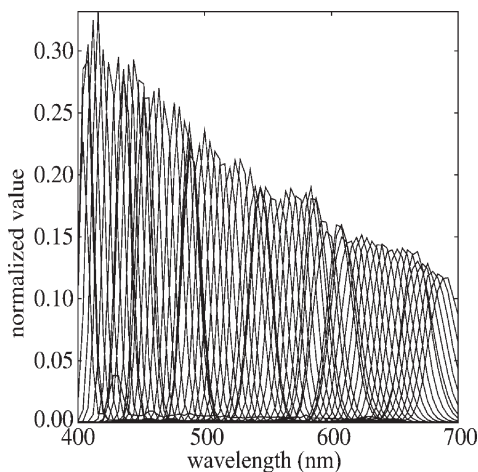


Figure 1. Spectral-sensitivity functions of the spectral camera system.

observe the scene illumination. First, we estimate spectral radiance from the camera outputs. Under the narrow-band assumption for each sensor, the spectral radiance is estimated in the form $Y_k(x) = p_k(x)/R_k$ ($k=1, 2, \dots, 69$), where $p_k(x)$ is the camera output at spatial location x and R_k is the sensor impulse response of k -th channel. We use the gray-world assumption. Then, the illuminant spectra is roughly estimated as the average spectral radiance \bar{Y}_k over the entire location x .

However, peak detection using the average spectral radiance is not always stable.

This average curve has no sharp peaks, so that the peak positions do not exactly correspond to the wavelengths of the fluorescent peaks. This is because the spectral sensitivity functions of the spectral camera are not ideal narrow bands. In order to detect spiky peaks on illuminant spectra, we propose use of the second derivative of the spectral camera outputs. The first derivative, called the gradient, calculates a slope of the spectral curve at each channel wavelength. The second derivative, called the Laplacian, calculates the divergence of the gradient of the spectral curve.

Experimental results

We have performed an experiment using the MacBeth Color Chart (shown) with the Mellow 5D as a light source. Figure 2 shows all

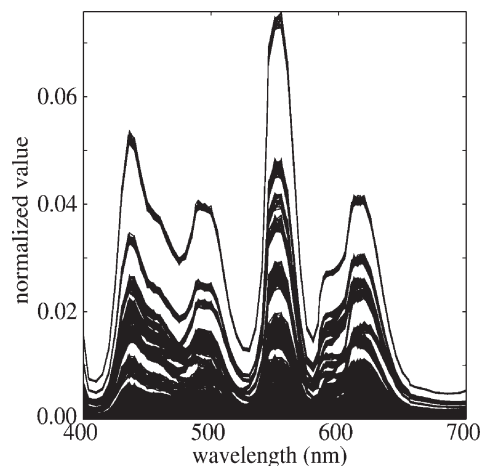


Figure 2. Outputs of the spectral camera with 69 channels for the Macbeth Color Chart under Mellow 5D illumination.

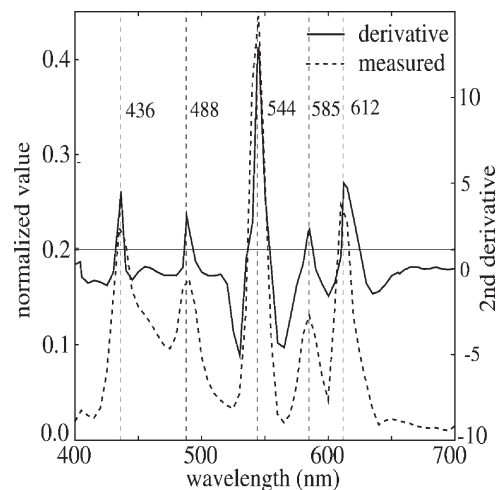


Figure 3. Average of the second-derivative spectra for all camera outputs.

outputs of the 69-channel spectral camera: there are no clear peaks. We therefore take the second-derivative spectra for all camera outputs. Figure 3 shows the average curve of the second derivatives. Sharp peaks are clearly generated, and the respective peak positions are coincident with the original fluorescent wavelengths on the measured illuminant spectrum

Continues on page 8.

Challenges in color reproduction: towards higher dimensions

Raja Bala, Principal Scientist, Xerox Imaging and Services Technology Center

Today's color management systems are largely based on pixel-wise processing of three-channel color data. We believe this simple representation does not adequately reproduce the color experience for the user, and that additional dimensions must be considered to more fully convey color information in imagery.

The spectral dimension

It is well known that a three-channel colorimetric representation does not fully capture the information necessary to reproduce color across different viewing conditions. Therefore, one approach that should be considered when discussing higher dimensions of color is using a spectral representation. However, it is important to distinguish between spectral representation for color measurement vs. spectral representation of images.

With regard to spectral measurement, today a variety of instruments offer different capabilities ranging from single-channel densitometers to three-channel colorimeters to spectrophotometers that measure 30 or more narrowband channels. The use of narrowband reflectance spectra can significantly improve the accuracy of color modeling and characterization, especially for printers.¹ Additionally, the necessary instrumentation has become more affordable and convenient to use over time: we can therefore expect that spectral measurement will become more commonplace in mainstream color-management applications.

Spectral representation of image data (so-called *spectral imaging*) has also been of much

interest. The main touted advantage is the elimination of metamerism (change of color in different conditions), but the technique also reduces bandwidth requirements by exploiting the fact that most naturally-occurring spectra are smooth, and thus adequately represented by a few (three to eight) basis functions.² There have been substantial research efforts both in the capture and reproduction of multispectral images and,³ in the standards arena, the CIE has devoted a technical committee to the topic of spectral imaging.

Despite the attention that has gone into this area, it has not made its way into mainstream imaging applications. We feel that this is because the cost of spectral image capture and reproduction is only worth the benefits gained for a few niche applications that are intolerant to metamerism artifacts, e.g. artwork reproduction.³

The spatial dimension

It has long been known that human color perception is strongly affected by spatial context. This effect is predicted to some extent by color appearance models such as CAM02.⁴ However, such classic models are only applicable under certain restrictive conditions and do not adequately predict the appearance of complex images. We are beginning to see attempts to predict image appearance, as with the image color-appearance model (iCAM).⁵ The CIE has also devoted technical committees towards the development of color-appearance and -difference models that can be applied towards com-

plex images.

Typical color mappings, however, are essentially still pixel-wise operations. The transforms are derived using metrics based only on color coordinates, and do not account for the spatial structure of the image. A classic example is gamut-mapping, where the algorithm that minimizes a pixelwise color-difference metric often results in loss of texture and edge information.⁶

We have developed a simple framework to incorporate a spatial component in color mappings, as depicted in Figure 1. In this framework, T is a standard pixel-wise color mapping, such as a gamut-mapping operation. To restore important spatial information lost by T , a difference is taken between the input and mapped image in a suitable space, governed by function f_1 . The difference image is processed through a spatial filter H that only retains certain frequency bands of interest. The filtered difference image is then re-inserted into the transformed image after post-processing denoted by f_2 . This framework has been successfully used for color gamut mapping⁶ and color-to-grayscale mappings.⁷

A related application that benefits from spatial processing is the reproduction of high-dynamic-range (HDR) images, which typically requires compression from a dynamic range of 10000:1 for the scene to approximately 300:1 for a standard display. Here, too, there has been an evolution from pixel-wise tone mapping (or

Continues on page 10.

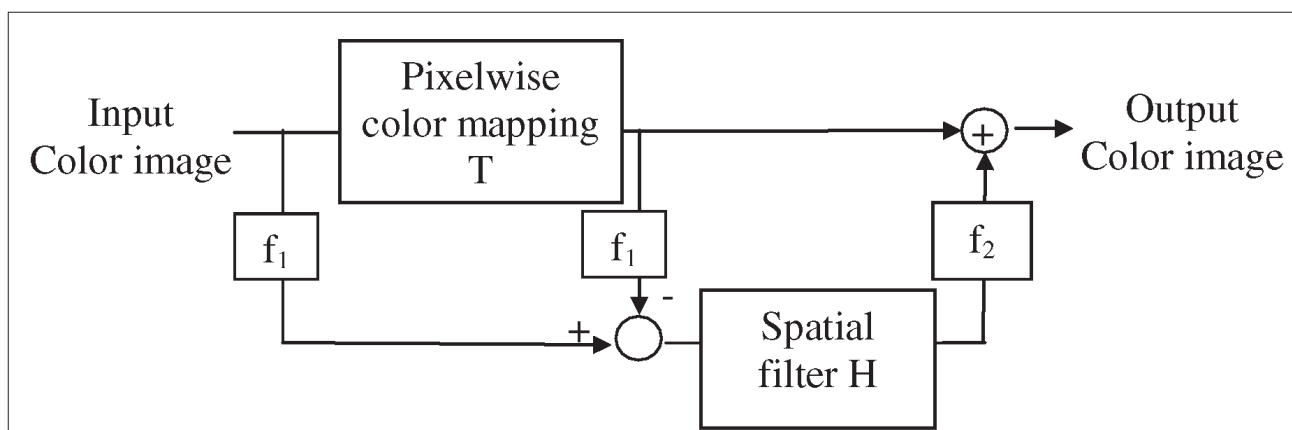


Figure 1. A simple model for introducing spatial context into a color mapping.

Effects of spectral information changes on spatial color computation

Alessandro Rizzi, Davide Gadia, and Daniele Marini, Università degli Studi di Milano

Color sensation comes from the interaction between spectral light distributions and surface reflectances. To produce this sensation, an observer (real or electronic) is needed and either color matching functions (CMFs) or alternative integration curves have to convert continuous spectral information into a limited number of chromatic values (usually a triplet). Here we describe work intended to verifying the robustness of a computational model of spatial color appearance in relation to changes in the acquisition of spectral information.

The basic idea is that human vision is the result of evolution; it acquires visual information in a smart way and is robust against highly-varying observation conditions. Vision is not just a trivial acquisition of pixels: lightness and color sensations are the result of human vision system's ability to adapt and perform cortical 'computations' that make it a more versatile visual acquisition 'instrument'. In other words, spatial distribution of visual information in the scene strongly affects lightness and color appearance.

There are several models that accomplish spatial color computation: in this paper we will discuss Retinex,¹ since it is well-known in the imaging community and has been used to test changes in spatial color computation with varying illuminants and acquisition curves. In other word, we will investigate how robust Retinex is against linear and non-linear variation in the CMFs.

Test setup

We built a synthetic scene, similar to the Cornell box,² containing a simplified MacBeth-like color checker that uses a photometric ray tracer. This program can manage the spectral characterization of light, materials, and their interaction in a scene, and produce a multispectral image as an output. This has, for each pixel, all the information about the spectral high-dynamic-range (HDR) luminance distribution with a precision of 5nm.

Synthetic HDR multispectral images of scenes are generated using two illuminant sets: the first has two D65 lights, while the second has one A and



Figure 1. False color image of the synthetic test scene.

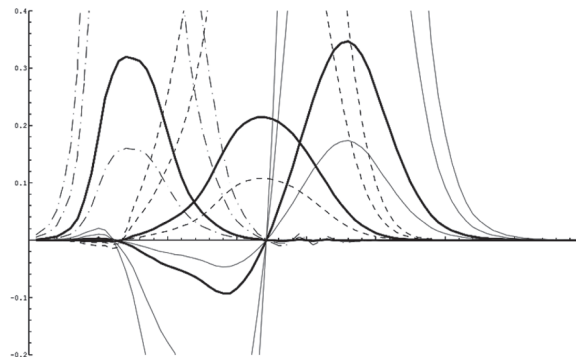


Figure 2. Examples of standard (black) and linearly modified CMFs (shades of gray).

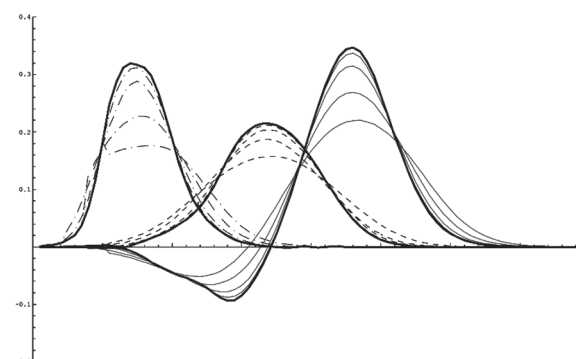


Figure 3. Examples of standard (black) and non-linearly modified CMFs (shades of gray).

one C illuminant. From these two scenes we generated a set of high-dynamic-range RGB images from a single viewpoint, using standard and modified CMFs. A false color image is shown in Figure 1.

The CMFs were modified linearly by dividing or multiplying each point of the curve for the same constant value, or non-linearly by substituting each value in the curve with mean-of-neighbor curve values (moving an average of 5 to 21 values). Examples of standard and linearly-modified CMFs are shown in Figure 2.

The HDR images, computed with regular and modified CMFs, were converted to standard RGB images using first a linear tone-mapping (TM) algorithm, and then an algorithm based on Retinex.³

Test results

Two kind of CMF curve variations were tested: linear and non-linear.

In Table 1 we present the mean ΔE in CIELab, computed over all pixels, for each couple of images. They were rendered under D65 illuminants after linear manipulation of RGB CMF curves by factors of 0.5 \times , 4 \times , and 8 \times . Just one CMF was modified at a time. In Table 2 we present the same results for the scene under illuminants A and C.

The linear tone map only represents the physical computation of light distribution, while the Retinex tone map performs a chromatic and lightness spatial adjustment. Retinex strongly compensates the CMFs linear variations.

To simulate nonlinear variations of the CMFs we applied a moving average of 5, 9, 15, and 21 neighboring points to each curve. The resulting CMFs are shown in Figure 3. In Tables 3 and 4 we present the same measures as in Tables 1 and 2, but with the nonlinear changes in CMFs. It is clear that, in this case, the effects are quantitatively less uniform and more sensitive to illuminant changes.

As a preliminary comment, based only on the tests described above, variation of CMFs seems to have more effect on physical color computation, while spatial color computation seems to normalize this effect: Retinex tone-maps images towards

Continues on page 9.

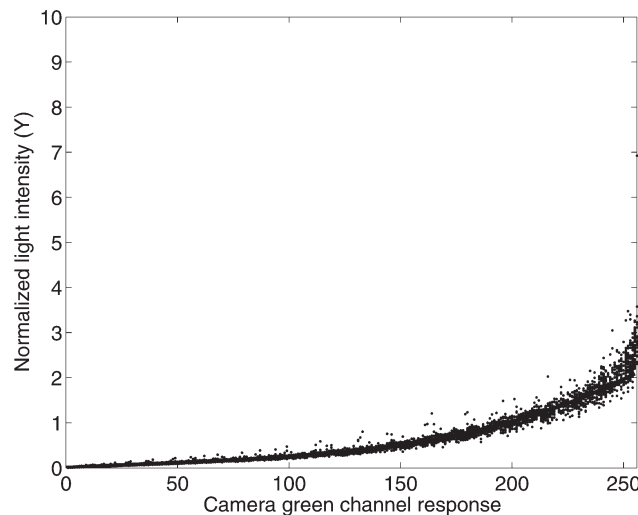
Acquiring and calibrating a large-dynamic-range image database of natural scenes

Fuhui Long, Center for Cognitive Neuroscience, Duke University; Hanchuan Peng, Life Sciences Division, Lawrence Berkeley National Laboratory

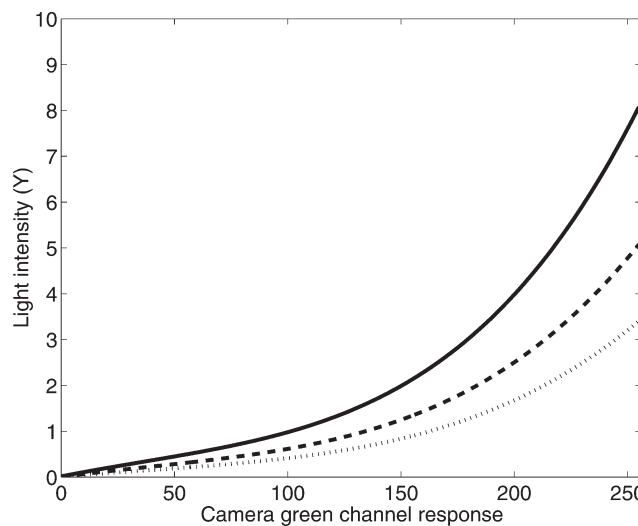
A large database of natural images that have a large dynamic range and have not been distorted by the imaging process is essential to human vision research. We recently acquired a database of natural scenes containing 1600 images taken using the Olympus C2040 digital camera. We carefully corrected for spatial falloff, non-linearity, spectral bias, blurring, and noise, and used multiple exposures to acquire a large dynamic range for each image.

Spatial falloff—caused by the cosine 4th law and by vignetting inherent in most digital cameras¹—refers to the fact that pixel intensity attenuates as the distance between the pixel and the image center increases. We corrected this by taking images of a uniformly-illuminated Macbeth white-balance card that filled the camera's entire field of view. By computing the ratio between the intensity of a given pixel and the average intensity of pixels in the central 2% of the image, we were able to obtain a function that describes the attenuation coefficient at each pixel. We then correct spatial falloff by dividing the intensity of each pixel with its corresponding coefficient. This process was repeated for each aperture and focal length used when acquiring the database.

Responses in the red, green, and blue channels of the Olympus C2040 are nonlinear functions of the incident light intensity. To recover the linear relationship, we uniformly illuminated the standard Macbeth color checker in stable sunlight. We then measured the RGB values and radiance spectrum of the same light reflected from each of the six gray patches of the checker with the digital camera (Olympus C2040) and a spectroradiometer (FieldSpec HandHeld, Analytical Spectral Devices Inc., Boulder, CO) respectively. This process was repeated at different times and on different days for each aperture and shutter speed used when acquiring the images. Taking a specific exposure setting as the reference, we then normalized all the measured data and used a polynomial fitting to generate a reliable function of the camera response. The response function for a spe-



(a)



(b)

Figure 1. Non-linearity calibration. *a)* Measured data (after normalization) under 88 exposure settings. Taken by pairing four *f*-stop values ranging from 2.6 to 8 and 22 shutter speed values ranging from 1/6s to 1/800s. The measurement at *f*7 and 1/160s was used as the reference for normalization. *b)* Camera-response functions for three exposure settings in the green channel: the solid line is *f*5.0, 1/400s; the dashed line *f*5.0, 1/250s; and the dotted line *f*5.0, 1/160s.

cific exposure was then generated from this systematic function by multiplying the corresponding ratios (see Figure 1). These functions thus map the camera responses of the RGB chan-

nels under each particular exposure setting into their true light intensity values.

Optical blurring was reduced by measuring the spatial point-spread functions of the camera and by conducting inverse filtering. To reduce the influence of noise, we frequently took dark images with camera cap on and subtracted the dark current from acquired scene images. The method we used to extend the dynamic range of the images also has the effect of reducing both noise and the blooming effect. The spectral sensitivity function was obtained by measuring narrow-band light (generated using a monochromator) reflected from the Macbeth white-balance card with the digital camera and the spectroradiometer respectively.²

In the database acquisition stage, we fixed all the remaining settings of the camera except for the shutter speed, aperture, and zooming factor. Particularly, we disabled the auto white-balancing function of the digital camera and manually set the Macbeth white balance card—illuminated under a typical sunlight at noon—as the white reference. We fixed this reference throughout image acquisition and calibration. After several images were acquired, we took an image of the Macbeth white balance card, illuminated under the same lighting conditions, in order to provide the white point for modeling chromatic adaptation in human vision in later statistical analysis of the database.

To extend the dynamic range of the images, we took five images of the same scene under stable sunlight with different exposure settings (determined by the combination of shutter speed and aperture), each differing by one stop. The middle one was determined by the exposure automatically measured by the camera. With these images and the camera response functions of the corresponding exposures, we used linear-weighted summation to combine the five images into a single high-dynamic-

Continues on page 10.

Spectral sensitivity functions for humans and imagers: 1861 to 2004

Continued from cover.

than the red-cyan scale. Vision compensates for spectral overlap by post-receptor processing. In the visually-isotropic Munsell Color Space, the distance between maximum red (5R5/14) and maximum cyan (5BG 5/10) is equivalent to 12 lightness steps. However, white to black has only eight steps of the equivalent size. In appearance, the range of chromatic colors is greater than that of achromatic colors. Vision overcompensates for crosstalk and stretches the chroma of cone responses.

Departures from perfect color constancy

Color constancy experiments show that the appearance of objects is almost constant with spectral changes in illumination. These experiments are one of many that discredited the idea that human color vision mimics film. Color is *not* uniquely determined by the quanta catch of cone receptors.

As the explanation of constancy, von Kries suggested that changes in spectral illumination caused relative changes in receptor sensitivities (called adaptation).³ Incomplete-adaptation hypotheses assume that the departures from perfect constancy are the result of imperfect adjustments to changed illumination. Since incomplete adaptation hypothesis is controlled only by illumination changes, it predicts that gray and red papers will have identical constancy departures.

Spatial comparisons

The 1960s saw the start of three major bodies of work establishing that vision is controlled by a

number of independent channels using spatial comparisons. Hubel and Wiesel's neurophysiology of the visual cortex,⁴ Fergus Campbell's psychophysics of spatial-frequency channels,⁵ and Edwin Land's Retinex theory⁶ of color, all established that vision works by spatial comparisons. Retinex uses these within a color channel to establish relationships across the entire image, then it compares the three color channels to generate appearance. Here, relative quanta catch within a channel is more important than quanta catch at a pixel.

Recent studies⁷ of the departures from perfect constancy highlight the role of crosstalk. In Retinex, the long-wave output calculation uses the ratio of the red paper to the white paper. This ratio changes with relative changes in 625nm, 530nm, and 455nm illumination because the proportions of crosstalk contributions change. This observation is true for colored papers, but not for achromatic ones. By definition, a gray paper has the same reflectance for all wavelengths. When the crosstalk component is the same as the principle component, then the ratio of gray to white is constant for all changes in illumination.² Again, parallel analyses hold for all color channels.

Recent experiments used 27 different combinations of 625nm, 530nm, and 455nm light. Matching data demonstrate that gray papers showed little change in matches, while colored papers show significant changes in appearance. Discrepancies from perfect constancy are consistent with three-channel sensor crosstalk in spatial comparisons. They are inconsistent with

incomplete adaptation.

In summary, image makers have opted for narrow, non-overlapping spectral sensitivities to minimize crosstalk. Humans—limited by the chemistry of visual pigments—use broad, overlapping sensitivities, with additional neural mechanisms that overcompensate for crosstalk. These post-receptor mechanisms generate color constancy using spatial comparisons.

John J. McCann

McCann Imaging

Belmont, MA

E-mail: mccanns@tiac.net

References

1. F. E. Ives, *A New Principle in Heliography*, self-published Philadelphia, 1889.
2. J. J. McCann, S. McKee, and T. Taylor, *Quantitative studies in Retinex theory: A comparison between theoretical predictions and observer responses to 'Color Mondrian' experiments*, *Vision Res.* **16**, pp. 445-458, 1976.
3. G. Wyszecki and W. S. Stiles, *Color Science: Concepts and Methods, Quantitative Data and Formulae, 2nd Ed*, John Wiley & Sons, New York, pp. 429-451, 1982.
4. D. Hubel and T. Wiesel, *Receptive fields and functional architecture of monkey striate cortex*, *J. Physiol.* **195** (1), pp. 215-243, 1968.
5. F. W. Campbell and J. G. Robson, *Application of Fourier analysis to the visibility of gratings*, *J. Physiol.* **197** (3), pp. 551-566, 1968.
6. E. H. Land, *The Retinex*, *Am. Scientist* **52**, pp. 247-264, 1964.
7. J. J. McCann, *Mechanism of Color Constancy*, *Proc. IS&T/SID Color Imaging Conf.*, IS&T, Scottsdale, Arizona, in press, 2004.

Estimation of fluorescent scene illuminant

Continued from page 4.

(shown in the broken curve in Figure 3). Thus, the second-derivative spectrum is effective for fluorescent-peak detection.

This method was applied to a database of twelve fluorescent light sources (F1, F2, ..., F12 defined by CIE³) and six real fluorescent lamps from products on the market. As a result, all the fluorescent spectral curves can be roughly classified into three groups. The first group (F1-F9), which we call the CIE standard type, has main peaks at 436nm, 544nm, and 580nm. The second group, the tri-band type (F10-F12) has its strongest lines at 436nm, 488nm, 544nm, and 612nm. Finally, the third group—the incandescent type—has its peaks at 436nm, 544nm, and 656nm.

Shoji Tominaga

Department of Engineering Informatics
Osaka Electro-Communication University
Osaka, Japan
E-mail: shoji@tmlab.osakac.ac.jp

References

1. S. Tominaga and B.A. Wandell, *Natural scene illuminant estimation using the sensor correlation*, *Proc. of The IEEE* **90** (1), pp. 42-56, 2002.
2. S. Tominaga, S. Ebisui, and B.A. Wandell, *Scene illuminant classification: Brighter is better*, *J. Opt. Soc. Am. A.* **18** (1), pp. 55-64, 2001.
3. CIE, *Colorimetry*, Publication CIE 15.2, 1986.

Spectral imaging at Chiba University

Continued from page 3.

plication will be revealed in the future. This is a great opportunity for young scientists and laboratories to contribute to the research and development of multispectral imaging.

Prof. Yoichi Miyake

Director of Research Center for Frontier Medical Engineering
Chiba University, Japan
E-Mail: miyake@faculty.chiba-u.jp
<http://www.mi.tj.chiba-u.jp/~miyake/>
<http://www.cfme.chiba-u.jp/>

Effects of spectral information changes on spatial color computation

Continued from page 6.

similar ΔE values in all cases. For a more detailed analysis, see Reference 4.

Alessandro Rizzi, Davide Gadia,* and Daniele Marini†

Dipartimento di Tecnologie dell'Informazione
Università degli Studi di Milano, Italy
E-mail: rizzi@dti.unimi.it

*†Dipartimento di Informatica e Comunicazione
Università degli Studi di Milano, Italy
E-mail: *gadia@dico.unimi.it
E-mail: †daniele.marini@unimi.it

References

1. E. Land and J. McCann, *Lightness and Retinex Theory*, *J. of Optical Society of America* **61**, pp. 1-11, 1971.
2. <http://www.graphics.cornell.edu/online/box/>
3. D. Gadia, D. Marini, and A. Rizzi, *Tuning Retinex for HDR Images Visualization*, **CGIV04, IS&T Second European Conf. on Color in Graphics, Imaging and Vision**, pp. 326-331, 2004.
4. A. Rizzi, D. Gadia, and D. Marini, *Spectral information and spatial color computation*, to be presented at **Color Imaging: Processing, Hardcopy, and Applications in IS&T-SPIE Electronic Imaging 2005**, San Jose, January 2005.

Table 1. Mean ΔE in CIELab for images under D65, after linear manipulation of CMFs curves by 0.5x, 4x, and 8x.

Linear changes	R	G	B
Linear TM	47.04	65.54	67.55
Retinex TM	4.51	4.52	4.51

Table 2. Mean ΔE in CIELab for images under A and C, after linear manipulation of CMFs curves by 0.5x, 4x, and 8x.

Linear changes	R	G	B
Linear TM	45.81	60.48	56.13
Retinex TM	4.55	4.55	4.55

Table 3. Mean ΔE in CIELab for images under D65, after non-linear transformation of CMFs curves with 5, 9, 15, and 21 moving averages.

Non-linear changes	R	G	B
Linear TM	0.70	1.32	3.53
Retinex TM	5.62	4.56	4.54

Table 4. Mean ΔE in CIELab for images under A and C, after non-linear transformation of CMFs curves with 5, 9, 15, and 21 moving averages.

Non-linear changes	R	G	B
Linear TM	1.10	1.26	0.97
Retinex TM	4.56	4.67	4.71

Calendar

2005

IS&T/SPIE International Symposium Electronic Imaging 2005

16-20 January
San Jose, California USA

Program • Advance Registration Ends
16 December 2004
Exhibition
electronicimaging.org/program/05/



SPIE International Symposium Medical Imaging 2005

12-17 February
San Diego, California USA

Program • Advance Registration Ends 3 February 2005
Exhibition
spie.org/conferences/programs/05/mi/



IS&T Archiving Conference 2005

26-29 April
Alexandria, Virginia USA

SPIE is a cooperating organization
Program
imaging.org/conferences/archiving2005/



Visual Communications and Image Processing (VCIP 2005)

12-15 July
Beijing, China

SPIE is a cooperating organization
Program
research.microsoft.com/asia/VCIP2005/

Optics & Photonics 2005 SPIE 50th Annual Meeting

31 July-4 August
San Diego, California USA

Call for Papers • Abstracts Due 17 January 2005
Exhibition
spie.org/conferences/calls/05/am/



The Fourth International Symposium on Multispectral Image Processing and Pattern Recognition (MIPPR)

31 October-2 November
Wuhan, China

SPIE is a Technical Cosponsor and will publish the proceedings.
Program
liesmars.wtusm.edu.cn/MIPPR2005/index.html

For More Information Contact

SPIE • PO Box 10, Bellingham, WA 98227-0010
Tel: +1 360 676 3290 • Fax: +1 360 647 1445
E-mail: spie@spie.org • Web: www.spie.org

Challenges in color reproduction: towards higher dimensions

Continued from page 5.

quantization) operators to more sophisticated models such as iCAM⁵ and Retinex⁸ that employ spatial operators to preserve local and global image contrast.

The goniometric dimension

Goniometry can play an important role in color perception. The computer graphics community has long been using gloss models in the realistic rendering of synthetic color images. In the area of color appearance, studies have shown that at non-specular viewing angles, the perceived chroma of a color stimulus increases with its gloss.⁹ This agrees with our common experience when viewing glossy vs. matte photographic prints.

Despite recognition of the importance of goniometry, not much progress has been made towards incorporating it into mainstream color-reproduction applications. Perhaps among the first efforts to consider the goniometric aspect in a classic color management application is the work by Patil et al.,¹⁰ wherein a gloss model is incorporated into a color softproofing application. The user is able to move a softproof of a color image in three dimensions on the display, and can visualize the effect of gloss on the image. Experiments indicate that gloss could be an important cue in bridging the gap between softcopy and hardcopy media. This is a significant first step in incorporating goniometry into standard color management operations.

In conclusion, when one thinks about the higher dimensions of color reproduction, there is a natural proclivity to consider the spectral aspect. This paper challenges this notion, proposing instead that while a spectral representation is useful for color measurement and modeling, greater benefit for mainstream color imaging can be gained by considering other dimensions, such as spatial context and image goniometry. The recent work on spatial mappings and 3D softproofing marks the inception of efforts to incorporate these additional dimen-

sions into classic color management operations. Interestingly, these approaches often compromise pixel-wise color accuracy, and yet produce superior perceived image quality. This reiterates the fact that color perception goes beyond colorimetric matching, and this is especially true when no original is present.

Raja Bala

Principal Scientist
Xerox Imaging and Services Technology Center
Webster, NY
E-mail: rbala@crt.xerox.com
http://chester.xerox.com/~raja

References

1. G. Sharma, **Digital Color Imaging Handbook**, CRC Press, Boca Raton, 2003.
2. M. Vrhel et al., *Measurement and analysis of object reflectance spectra*, **Color Res. Appl.** **19** (1), pp. 4-9, 1991.
3. L. W. MacDonald and M. R. Luo, Ed., **Colour Imaging—Vision and Technology**, Wiley, Chichester, UK, 1999.
4. N. Moroney et al., *The CIECAM02 color appearance model*, **Proc. IS&T/SID's 10th Color Imaging Conf.**, pp. 23-27, 2002.
5. M. Fairchild and G. Johnson, *Meet iCAM: A next-generation color appearance model*, **Proc. IS&T/SID's 10th Color Imaging Conf.**, pp. 33-38, 2002.
6. R. Balasubramanian et al., *Gamut mapping to preserve spatial luminance variations*, **Proc. IS&T and SID's 8th Color imaging Conf.**, pp. 122-128, 2000.
7. R. Bala and R. Eschbach, *Spatial color-to-grayscale conversion preserving chrominance edge information*, **Proc. IS&T/SID's 12th Color Imaging Conf.**, 2004.
8. R. Sobol, *Improving the Retinex algorithm for rendering wide dynamic range photographs*, **Proc. SPIE 4662**, pp. 341-348, 2002.
9. E. Dalal and K. Natale-Hoffman, *The effect of gloss on color*, **Color Research & Appl.** **24** (5), pp. 369-375, 1999.
10. R. Patil et al., *3D simulation of prints for improved softproofing*, **Proc. IS&T/SID's 12th Color Imaging Conf.**, 2004.

Acquiring and calibrating a large-dynamic-range image database of natural scenes

Continued from page 7.

range image.³

Fuhui Long and Hanchuan Peng*

Center for Cognitive Neuroscience
Duke University, Charlotte, NC
E-mail: long@neuro.duke.edu
*Life Sciences Division
Lawrence Berkeley National Laboratory
Berkeley, CA
E-mail: hpeng@lbl.gov

References

1. N. Asada, A. Amano, and M. Baba, *Photometric calibration of zoom lens systems*, **Proc. of IEEE Int'l Conf. on Pattern Recognition**, pp.189-190, 1996.
2. P. L. Vora, J. E. Farrell, Tietz, J. D., and D. H. Brainard, *Digital color cameras. Spectral response*, **Hewlett-Packard Laboratory Technical Report HPL-97-54**, 1997.
3. P. E. Debevec and J. Malik, *Recovering high dynamic range radiance maps from photographs*, **SIGGRAPH'97**, pp. 369-378, 1997.

Segmentation for mixed raster contents

Continued from page 12.

coded as foreground layers. Many existing segmentation algorithms (such as those described in References 2 and 3) can be used directly with little modification. In the second step, only those objects that can be represented by a constant color without introducing significant visual artifacts are selected for further foreground encoding. To test for this, the color uniformity and geometric characteristics of a few features are measured for each object. Conventional color-uniformity measures may not yield the best results for this application, as most objects will be small and composed of thin strokes: such objects tend to contain a higher percentage of edge pixels with higher-than-average noise content.

As a result, the color uniformity test we propose tries to measure only the interior of the object, ignoring the edge pixels. In addition, the test requires less-strict color uniformity for smaller and thinner objects. The objects that are chosen are clustered in color space as the third step. Many objects are composed of similar colors. For example, the characters in a word, a line, a paragraph, or even an entire page may share the same original color. Although their color measurements after printing and scanning may deviate from the original, their differences typically remain small. We often do not have the luxury of coding such objects into different foreground layers. Grouping them into one or several clusters and representing each in a single foreground layer is usually sufficient. The color similarity measure we use for clustering again takes into consideration that most objects are small and thin. To enhance clustering accuracy and efficiency, we also use object location and structure information. In the final step, the image is segmented so that each foreground layer encodes the objects from one color cluster.

This algorithm has been extensively tested with many different types of image.

Zhigang Fan and Timothy Jacobs

Xerox Corporation
Webster, NY
E-mail: {Zfan, Tjacobs}@crt.xerox.com

References

1. Draft Recommendation T.44, *Mixed Raster Content (MRC)*, **ITU-T Study Group 8, Question 5**, May 1997.
2. Z. Fan and M. Xu, *A simple Segmentation Algorithm for Mixed Raster Contents Image Representation*, **Proc. SPIE 4663**, pp. 63-71, 2002.
3. H. Cheng and Z. Fan, *Background Identification Based Segmentation and Multilayer Tree Based Representation of Document Images*, **Proc. ICIP**, pp. 1005-1008 Sep. 2002.

Join the SPIE/IS&T Technical Group

...and receive this newsletter

This newsletter is produced twice yearly and is available only as a benefit of membership of the SPIE/IS&T Electronic Imaging Technical Group.

IS&T—The Society for Imaging Science and Technology has joined with SPIE to form a technical group structure that provides a worldwide communication network and is advantageous to both memberships.

Join the Electronic Imaging Technical Group for US\$30. Technical Group members receive these benefits:

- *Electronic Imaging* Newsletter
- SPIE's monthly publication, *oemagazine*
- annual list of Electronic Imaging Technical Group members

People who are already members of IS&T or SPIE are invited to join the Electronic Imaging Technical Group for the reduced member fee of US\$15.

Please Print Prof. Dr. Mr. Miss Mrs. Ms.

First (Given) Name _____ Middle Initial _____

Last (Family) Name _____

Position _____

Business Affiliation _____

Dept./Bldg./Mail Stop/etc. _____

Street Address or P.O. Box _____

City _____ State or Province _____

Zip or Postal Code _____ Country _____

Phone _____ Fax _____

E-mail _____

Technical Group Membership fee is \$30/year, or \$15/year for full SPIE and IS&T Members.

Amount enclosed for Technical Group membership \$ _____

I also want to subscribe to IS&T/SPIE's *Journal of Electronic Imaging* (JEI) \$ _____
(see prices below)

Total \$ _____

Check enclosed. Payment in U.S. dollars (by draft on a U.S. bank, or international money order) is required. Do not send currency. Transfers from banks must include a copy of the transfer order.

Charge to my: VISA MasterCard American Express Diners Club Discover

Account # _____ Expiration date _____

Signature _____

(required for credit card orders)

Reference Code: 3995

JEI 2004 subscription rates (4 issues):

Individual SPIE or IS&T member*

U.S.

\$ 55

Non-U.S.

\$ 55

Individual nonmember and institutions

\$270

\$290

Your subscription begins with the first issue of the year. Subscriptions are entered on a calendar-year basis. Orders received after 1 September 2004 will begin January 2005 unless a 2004 subscription is specified.

*One journal included with SPIE/IS&T membership. Price is for additional journals.

Send this form (or photocopy) to:

SPIE • P.O. Box 10
Bellingham, WA 98227-0010 USA
Tel: +1 360 676 3290
Fax: +1 360 647 1445
E-mail: membership@spie.org

Please send me:

- Information about full SPIE membership
- Information about full IS&T membership
- Information about other SPIE technical groups
- FREE technical publications catalog

Electronic Imaging

The *Electronic Imaging* newsletter is published by SPIE—The International Society for Optical Engineering, and IS&T—The Society for Imaging Science and Technology. The newsletter is the official publication of the International Technical Group on Electronic Imaging.

Editor/Technical Group Chair Gabriel Marcu
Technical Editor Sunny Bains
Editorial Assistant Stuart Barr
Managing Editor/Graphics Linda DeLano

Articles in this newsletter do not necessarily constitute endorsement or the opinions of the editors, SPIE, or IS&T. Advertising and copy are subject to acceptance by the editors.

SPIE is an international technical society dedicated to advancing engineering, scientific, and commercial applications of optical, photonic, imaging, electronic, and optoelectronic technologies.

IS&T is an international nonprofit society whose goal is to keep members aware of the latest scientific and technological developments in the fields of imaging through conferences, journals and other publications.

SPIE—The International Society for Optical Engineering, P.O. Box 10, Bellingham, WA 98227-0010 USA. Tel: +1 360 676 3290. Fax: +1 360 647 1445. E-mail: spie@spie.org.

IS&T—The Society for Imaging Science and Technology, 7003 Kilworth Lane, Springfield, VA 22151 USA. Tel: +1 703 642 9090. Fax: +1 703 642 9094.

© 2004 SPIE. All rights reserved.

EIONLINE

Electronic Imaging Web Discussion Forum

You are invited to participate in SPIE's online discussion forum on Electronic Imaging. To post a message, log in to create a user account. For options see **"subscribe to this forum."**

You'll find our forums well designed and easy to use, with many helpful features such as automated email notifications, easy-to-follow 'threads,' and searchability. There is a full FAQ for more details on how to use the forums.

Main link to the new Electronic Imaging forum:

<http://spie.org/app/forums/tech/>

Related questions or suggestions can be sent to forums@spie.org.



The International Society
for Optical Engineering

Segmentation for mixed raster contents with multiple extracted constant-color areas

Zhigang Fan and Timothy Jacobs, Xerox Corporation

Mixed raster contents (MRC)¹ is a powerful image-representation concept for achieving high compression ratios while maintaining high reconstructed image quality. The *multiple extracted constant color areas* (MECCA) model has several advantages including its ease of decomposition and its inherent text-enhancement and noise-reduction features. Here we present a segmentation algorithm for the MRC MECCA model. This is a four-step algorithm that finds uniform text and other uniform color objects that carry detail in an image and extracts this information to form foreground layers. First the text and objects are extracted from the image, then they are tested for color constancy, after which the objects that are chosen are clustered in color space. Finally, the page is segmented such that each foreground layer codes the objects from the same color cluster.

Different image classes require different levels of coding fidelity. When compressing text, for instance, it is important to preserve the edges. Once the text is binarized, its compression is typically lossless. For continuous-tone images where errors in high-frequency components are better masked, lossy compression is usually employed. The MRC model is particularly suitable for compressing compound images such as a scanned pages containing text and pictures. The MRC decomposes the raster into several image layers, each of which can be coded efficiently with standard single-purpose compression methods.

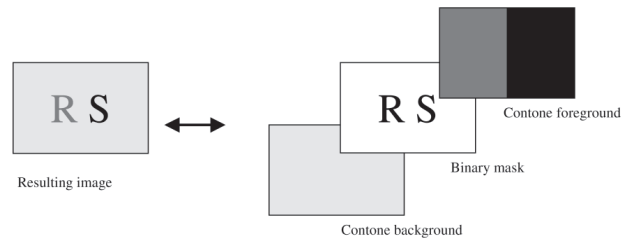


Figure 1. MRC Three-Layer Model.

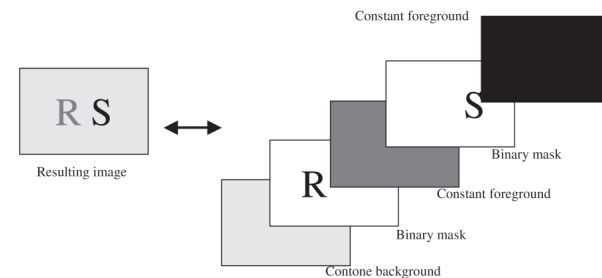


Figure 2. MRC MECCA Model.

The basic three-layer model is MRC's most common form. It represents the image as a binary mask and a contone foreground and background. The mask describes how to reconstruct the final images from the other two layers. When the mask pixel value is 1 (or 0), then the corresponding pixel from the foreground (or background) layer is selected for the final image (see Figure 1).

The three-layer model has the disadvantage that the resulting files, when coded as PDF, may not be printable on some Postscript and PDF

printers. This problem can be avoided if the decomposition contains only one contone layer, which is what the MECCA model does. It contains one contone background layer, N foreground layers, and N mask layers, where N is a non-negative integer, and the foreground layers are restricted to be constant colors (see Figure 2). Although constructing MECCA is computationally more difficult, the resulting PDF file is printable by almost all Postscript printers.

Segmentation is an essential part of implementing MRC-based coding. It generates the masks that decide the reconstruction rules. Segmentation is even more critical in a MECCA model than in a three-layer model. When an image is represented by a three-layer MRC, segmentation errors may reduce coding efficiency, but will typically not cause unacceptable image-quality degradation. However, in MECCA, anything represented in the foreground layers, typically text and details, must be quantized in color. This poses the risk that a segmentation error could lead to severe color damage. On the other hand, segmentation using MECCA can inherently enhance text/detail quality, resulting in sharpened edges and reduced noise.

The algorithm consists of four steps: object extraction, object selection, color clustering, and result generation. In the first step, text and other objects are extracted from the image. These objects are now candidates for being

Continues on page 10.

SPIE Society of Photo-Optical
Instrumentation Engineers

P.O. Box 10 • Bellingham, WA 98227-0010 USA

Change Service Requested

DATED MATERIAL

Non-Profit Org.
U.S. Postage Paid
Society of
Photo-Optical
Instrumentation
Engineers